ADVANCED MATERIALS

Communications

Solid-State Replication of Relief Structures in Semicrystalline Polymers**

By *Natalie Stutzmann, Theo A. Tervoort,* Cees W. M. Bastiaansen, Kirill Feldman,* and *Paul Smith*

Surface relief structures in polymers are employed in a large variety of useful objects such as compact discs, digital versatile disks, security and decorative holograms, brightness enhancement foils, and light collimators.[1–8] Original master relief structures, which often are produced with lithographic techniques and may feature dimensions in the micrometer and sub-micrometer range,[9,10] are reproduced into polymer materials with processes such as injection molding, hot embossing, and casting using metallic and inorganic masters, molds, or shims. Poly(methyl methacrylate), polystyrene, and polycarbonate are commonly used for the reproduction of relief structures with injection molding. Poly(ethylene terephthalate) and poly(vinyl chloride) are frequently employed in the reproduction of these structures in films with hot embossing, and special thermoset resins are available for casting.[11] Generally, amorphous polymers or polymeric materials of low crystallinity are used, and the actual reproduction of the relief structures is performed in the melt or in a pre-polymeric liquid state.[11]

Rather surprisingly, other members of the vast class of semicrystalline polymers are rarely employed for the production of relief structures, which may be associated with their perceived, often poor optical properties. However, various techniques exist to reduce light scattering in semicrystalline polymers and to produce highly transparent thin films.[12] Generally though, semicrystalline polymers offer advantages over amorphous macromolecular materials in that (above the glass transition temperature of the former) they are tough instead of brittle, and molecular orientation may be introduced and retained. The latter property leads to highly useful anisotropic optical characteristics as well as increased axial mechanical properties. In addition, certain semicrystalline polymers such as polyolefins and perfluorinated polymers are notorious for their non-adhesive properties to virtually all other materials, which represents a potentially significant asset in the reproduction of relief structures. Thus, we set out to investigate the feasibility of structuring the surfaces of semicrystalline polymers and explore some of the advantages alluded to above.

Here, in a first set of experiments, a perfluorinated polymer, poly(tetrafluoroethylene-*co*-hexafluoropropylene), FEP, was used as a model material. Hot embossing was performed in the polymer melt at 330 °C, after which the samples were quenched to room temperature. High-resolution optical micrographs, an environmental scanning electron micrograph, and scanning-probe micrographs of the embossed films are shown in Figure 1 together with the relief structures of the "master". As seen in these images, the relief structure of the latter is accurately reproduced in the polymer, even with respect to small details, such as an edge with a radius less than 10 nm. This holds promise for the generation of sub-micrometer and/or nano-sized structures. The reproduction of the microstructures and release of the sample from the master indeed appears to be facilitated by several factors: i) low adhesion between polymer and master, ii) substantial shrinkage (about 10 vol.-%) of the polymer during crystallization (mold release), and iii) the high toughness of the semicrystalline polymer (damage reduction). In general, the (isotropic) shrinkage upon crystallization may have an effect on the accuracy of reproduction, especially in case of free shrinkage. However, in our case, the shim was only removed after crystallization, and no effect on reproducibility was observed.

In particular the non-adhesive properties can, of course, be even further exploited. We used, for example, melt-embossed FEP films to produce epoxy "sub-masters", some with extremely fine features, as the scanning-probe micrographs (Fig. 2) illustrate. The epoxy replicas were obtained by pouring a pre-polymeric liquid onto the structured polymer, curing it at elevated temperature (60 °C) for 24 h and, subsequently, removing the epoxy sub-master from the embossed FEP film. The release from the microstructured polymer was straightforward, thus exemplifying that polymers such as perfluorinated polymers and polyolefins are not only highly suitable for replication but also for pattern transfer.

Generally, solid semicrystalline polymers are ductile in the temperature range between the glass transition and melting temperature. In a second set of experiments we attempted to hot emboss FEP in the solid state in this temperature range (T_{emb} = 200 °C). Gratifyingly, the microstructure of the master was reproduced over the entire area if somewhat higher pressures (up to 850 g/mm^2) were used in the experiments. Optical, environmental scanning electron, and scanning-probe microscopy revealed that the grating structure again is accurately reproduced in the films, indistinguishable from those shown in Figure 1 and,

[*] Dr. T. A. Tervoort, N. Stutzmann, K. Feldman, Prof. P. Smith
Department of Materials, ETH Zentrum
CH-8092 Zürich (Switzerland)
Dr. C. W. M. Bastiaansen
Polymer Laboratories, Eindhoven University of Technology
NL-5600 MB Eindhoven (The Netherlands)

[**] We thank Pauline Schmit for performing environmental scanning electron microscopy and Armin Schmid for his experimental work.

  0935-9648/00/0804-0557 $ 17.50+.50/0

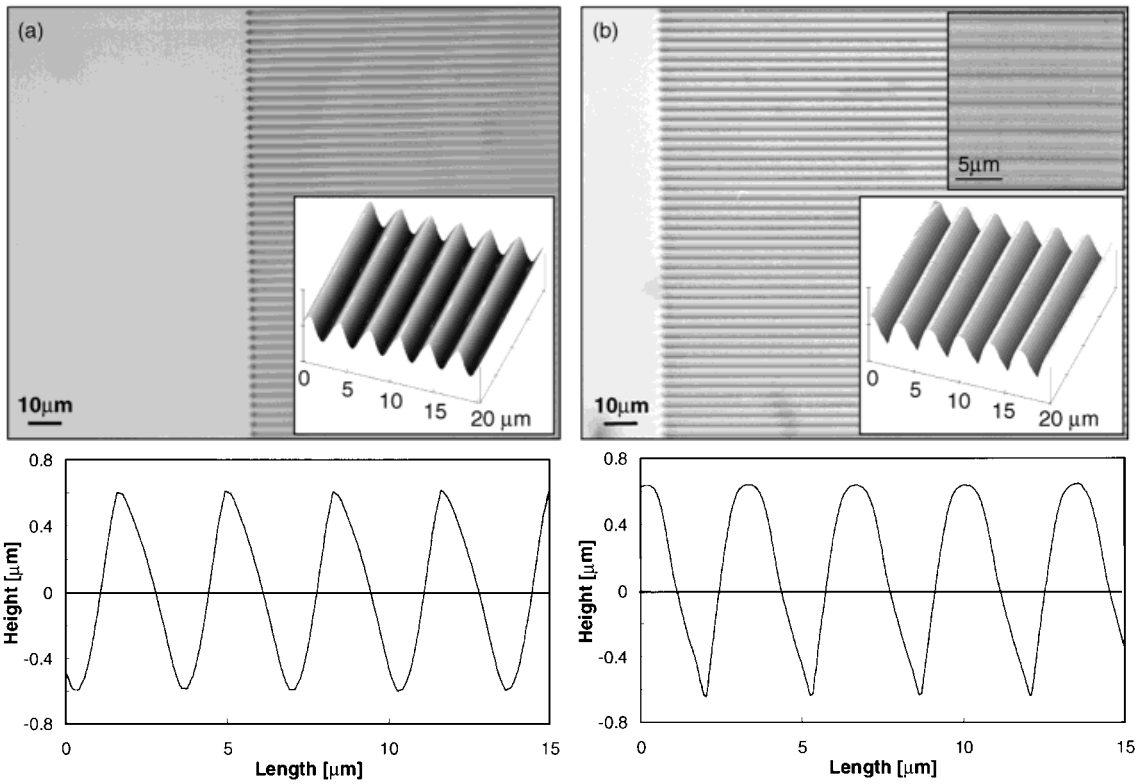

Fig. 1. High-resolution optical micrographs and scanning-probe micrographs (cross-section; three dimensional view as inset): a) of the master and b) of the poly(tetrafluoroethylene-*co*-hexafluoropropylene), FEP, relief structure. The second inset in (b) shows an environmental scanning electron micrograph of the melt-embossed structure.

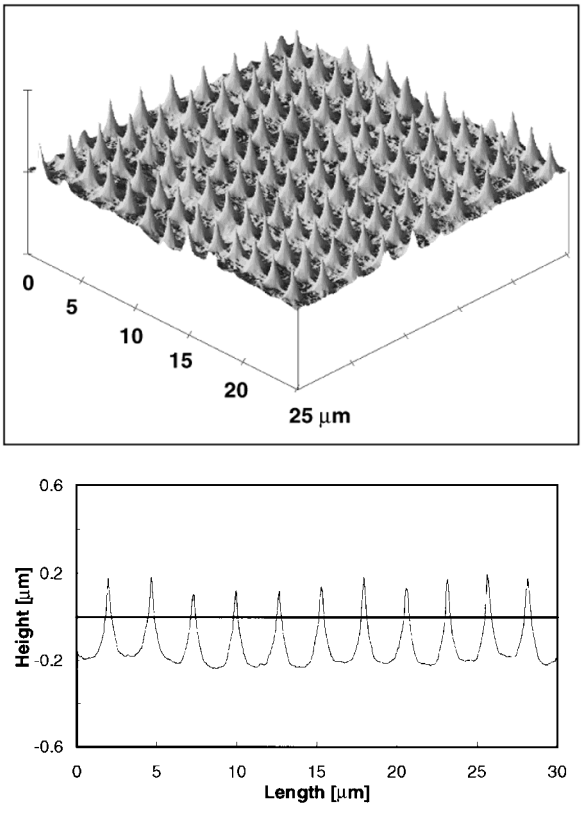

Fig. 2. Scanning probe micrographs (three-dimensional and cross-sectional view) of an epoxy-replica of a melt-embossed FEP film.

therefore, not reproduced here. Evidently, the high ductility of the polymer permits production of relief structures in the solid state, which opens interesting possibilities in the manufacturing of relief structures. For instance, re-embossing of relief structures in a pre-embossed, polymeric substrate can be performed. In order to demonstrate this option, a grating structure was first generated in the polymer melt and the sample was quenched to room temperature. The master was subsequently rotated 90° and the films were re-embossed in the solid state at 200 °C under a pressure of 300 g/mm^2, which yielded a final array of rectangular, pyramid-like features (Fig. 3a). The excellent regularity of the structure is demonstrated by its laser diffraction pattern (Fig. 3b). In the reference experiment, pre-embossed films were re-embossed in the polymer melt. The latter procedure invariably resulted in severe damage to the primary grating structure due to flow of the polymer, illustrating clearly that solid-state embossing is a pre-requisite for multiple embossing of relief structures in polymers. Although demonstrated here only for one particular geometry, it is self-evident that this technique allows for the generation of complex, multi-scale features.

In a third set of experiments, the concept of added molecular order was introduced in embossing by employing a highly anisotropic polymer. A uniaxially drawn (four times its original length), highly birefringent FEP film was used for this purpose. Special precautions were taken to obtain drawn films with smooth surface texture (see

  0935-9648/00/0804-0558 $ 17.50+.50/0

ADVANCED MATERIALS

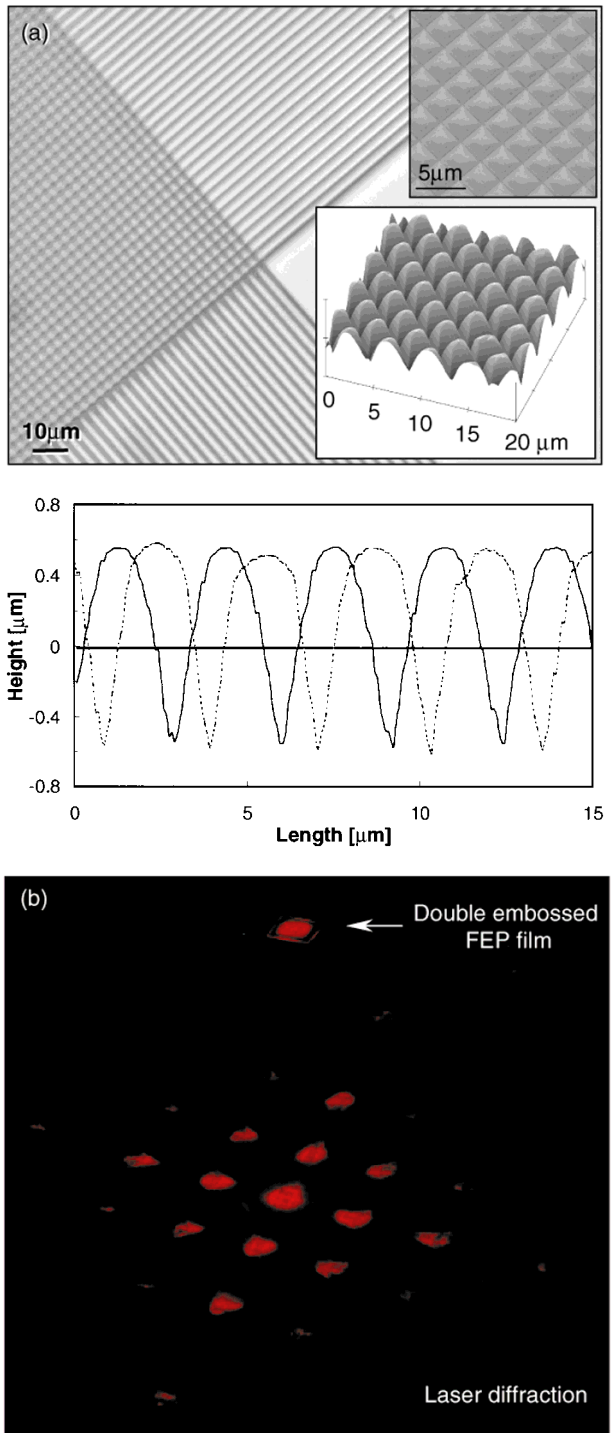

Fig. 3. Double-embossed relief structure. a) Bright field optical micrograph and scanning-probe micrograph (cross-sections of the first, melt-embossed structure, dashed line, and the in the solid-state, secondly embossed structure, solid line); the insets show a scanning-probe micrograph (three-dimensional view) and an environmental scanning electron micrograph. b) Laser diffraction pattern of the double-embossed structure.

experimental section). These films were embossed at 200 °C in the solid state: parallel, perpendicular, and at an angle of 45° to the drawing direction. Typical optical micrographs, environmental scanning electron micrographs, and scanning-probe micrographs of relief structures embossed parallel to the orientation direction and at an angle of 45° are shown in Figure 4. The corresponding micrographs of films embossed perpendicular to the drawing direction were virtually indistinguishable from Figure 4a, and are therefore not reproduced here. In all cases, well-defined gratings were obtained. Note the presence of the fibrillar features at an angle of 45° to the grating (Fig. 4b). The latter are of course associated with the uniaxial order in the FEP film used. These observations are indeed indicative of possibilities of generating materials that combine optical anisotropy originating from the bulk of an oriented polymer with other optical functionalities related to a relief structure.[13] In Figure 6, optical micrographs of relief structures embossed at an angle of 45° to the orientation direction are shown. The optical micrographs were recorded between crossed polarizers with the orientation direction of the drawn FEP parallel to one of the polarizers (Fig. 5a) and at an angle of 45° (Fig. 5b). The micrographs illustrate that a material with highly interesting optical properties results upon embossing a microstructure in an oriented polymer film, superimposing in this way a lamellar grating on a uniaxial birefringent material.

This unique optical behavior observed with light microscopy was further characterized using an experimental set-up as depicted schematically in Figure 6a. FEP films, embossed, parallel, perpendicular, and at an angle of 45° to the drawing direction, were positioned between crossed linear polarizers, with the drawing direction of the films aligned at an angle, θ, with respect to the analyzer. The transmitted light intensity of a white light source was subsequently measured with a highly sensitive photodiode as a function of the orientation angle, θ (Fig. 5c). In the inset of Figure 5c, moreover, the measured intensities for an unembossed film and a film embossed at an angle of 45° to the drawing direction are plotted in logarithmic scale to illustrate, in particular, the differences in the "low-intensity regime" clearly observed with light microscopy (Fig. 5a) between the unstructured and structured parts.

In order to model theoretically the optical performance of the microstructured, oriented film, we first applied the effective medium theory (EMT)[14] to estimate the optical properties of the embossed grating. Rigorously, EMT is only applicable to microstructures with sufficiently small features, i.e., with a grating period much smaller than the wavelength. Such subwavelength gratings only transmit the zeroth order (all other diffraction orders are evanescent) and will act as a homogenous birefringent material.[15–18] Therefore, they can be mathematically formulated as optical retarders, whereby EMT yields with simple birefringent film calculations the ordinary and extraordinary refractive index of this "artificially" induced birefringence, form birefringence.[19] We used, subsequently, Müller calculus[20] to describe the experimental system as a train of polarizers

  0935-9648/00/0804-0559 $ 17.50+.50/0

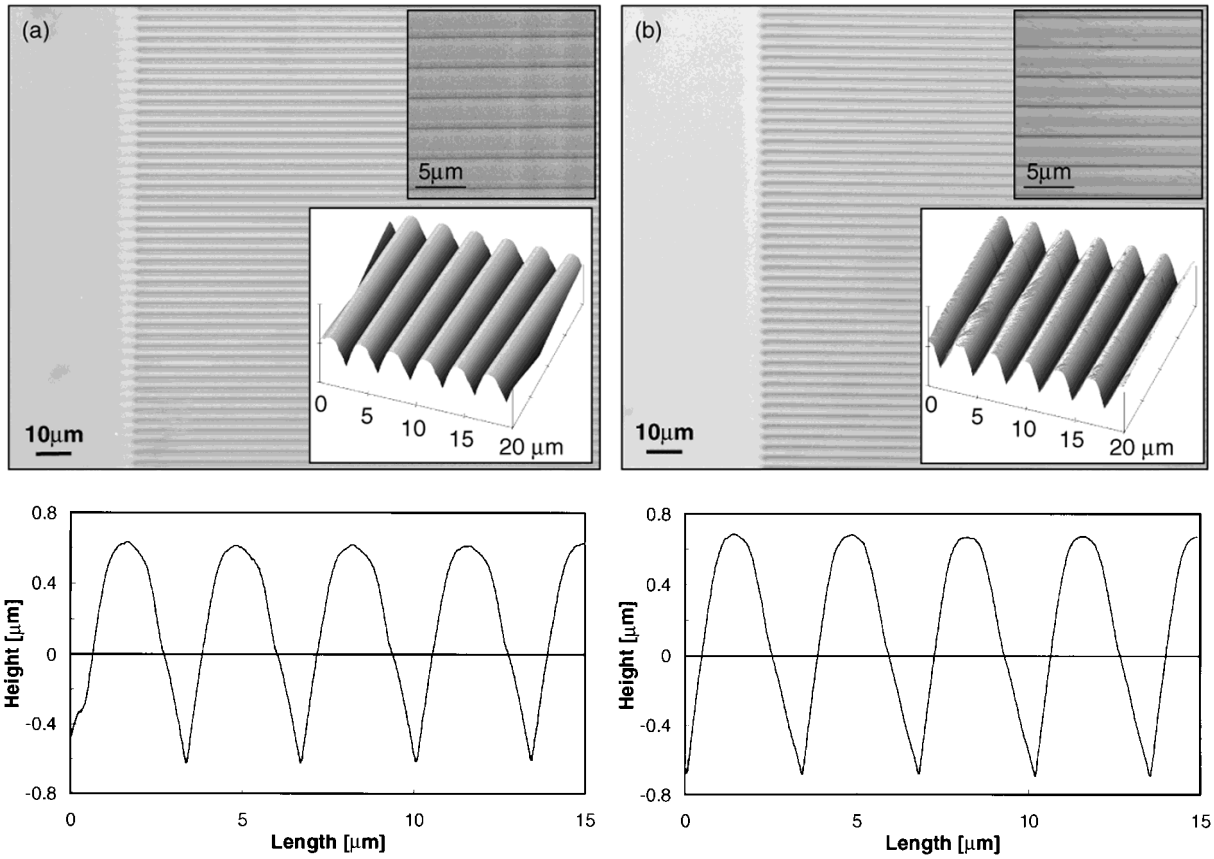

Fig. 4. Relief structures embossed in the solid state in oriented FEP. Optical and scanning-probe micrographs (cross-section) of: a) film embossed parallel to the orientation direction, and b) embossed at an angle of 45° to the orientation direction. The insets show corresponding scanning-probe micrographs (three-dimensional view) and environmental scanning electron micrographs.

and retarders (Fig. 6b) transmitting the incident, unpolarized light of intensity I_0, represented by the Stokes vector, S_0, with $S_0{}^T = (I_0, 0, 0, 0)$. The intensity of the exiting light is then given by the first component of the Stokes vector,[21] S.

$$S = M_{\text{polarizer2}} \times M_{\text{retarder2}} \times M_{\text{retarder1}} \times M_{\text{polarizer1}} \times S_0 \qquad (1)$$

The Müller matrices, $M_{\text{polarizer}}$, for the linear polarizers, $M_{\text{retarder1}}$, for the oriented FEP film, $M_{\text{retarder2}}$, for the grating, are as follows:

$$M_{\text{polarizer}} = 0.5 \cdot \begin{bmatrix} 1 & \cos[2\alpha] & \sin[2\alpha] & 0 \\ \cos[2\alpha] & \cos[2\alpha]^2 & \sin[2\alpha]\cdot\cos[2\alpha] & 0 \\ \sin[2\alpha] & \sin[2\alpha]\cdot\cos[2\alpha] & \sin[2\alpha]^2 & 0 \\ 0 & 0 & 0 & 0 \end{bmatrix}$$

$$M_{\text{retarder1}} = \begin{bmatrix} 1 & 0 & 0 & 0 \\ 0 & \cos[2\Theta]^2 + \sin[2\Theta]^2 \cdot \cos[\delta] & \sin[2\Theta]\cdot\cos[2\Theta]\cdot(1-\cos[\delta]) & -\sin[2\Theta]\cdot\sin[\delta] \\ 0 & \sin[2\Theta]\cdot\cos[2\Theta]\cdot(1-\cos[\delta]) & \sin[2\Theta]^2 + \cos[2\Theta]^2 \cdot \cos[\delta] & \cos[2\Theta]\cdot\sin[\delta] \\ 0 & \sin[2\Theta]\cdot\sin[\delta] & -\cos[2\Theta]\cdot\sin[\delta] & \cos[\delta] \end{bmatrix}$$

$$M_{\text{retarder2}} = \begin{bmatrix} 1 & 0 & 0 & 0 \\ 0 & \cos[2\Theta+\varphi]^2 + \sin[2\Theta+\varphi]^2 \cdot \cos[\delta] & \sin[2\Theta+\varphi]\cdot\cos[2\Theta+\varphi]\cdot(1-\cos[\delta]) & -\sin[2\Theta+\varphi]\cdot\sin[\delta] \\ 0 & \sin[2\Theta]\cdot\cos[2\Theta]\cdot(1-\cos[\delta]) & \sin[2\Theta+\varphi]^2 + \cos[2\Theta+\varphi]^2 \cdot \cos[\delta] & \cos[2\Theta+\varphi]\cdot\sin[\delta] \\ 0 & \sin[2\Theta+\varphi]\cdot\sin[\delta] & -\cos[2\Theta+\varphi]\cdot\sin[\delta] & \cos[\delta] \end{bmatrix}$$

Here, α describes the orientation of the polarizers (thus α = 0° for polarizer 1 and 90° for polarizer 2) and φ the angle of the grating with respect to the drawing direction of the polymer film. θ is the orientation angle as depicted in Figure 6a, and the retardance, δ, where

$$\delta = \frac{2\pi\Gamma}{\lambda} = \frac{2\pi\Delta n d}{\lambda}$$

with Γ = the retardation, Δn = the birefringence, and d = the thickness of the oriented film or grating. The calculations

0935-9648/00/0804-0560 $ 17.50+.50/0

ADVANCED MATERIALS

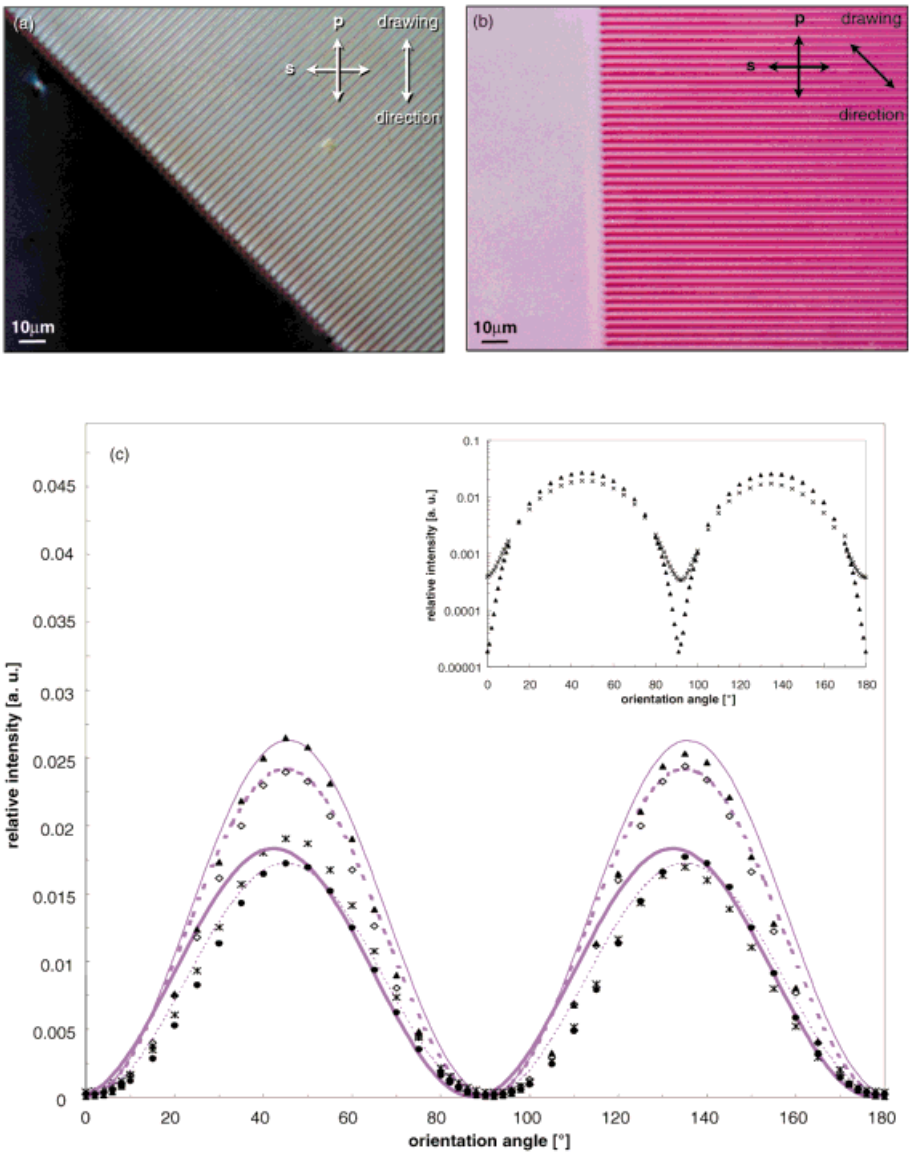

Fig. 5. Relief structure solid-state embossed in oriented FEP at an angle of 45° to the orientation direction. Optical micrographs recorded between crossed polarizers with: a) orientation direction of the drawn films parallel to one of the polarizers; b) at an angle of 45° to the polarizers. c) Optical characteristics (measured and curve fitted) of oriented films, embossed parallel, perpendicular and at an angle of 45° to the drawing direction; unembossed film, solid line (curve fitted) and ▲ (measured); film embossed parallel, dashed bold line (curve fitted) and ◇ (measured); film embossed perpendicular, dashed line (curve fitted) and ● (measured); film embossed at 45°, solid bold line (curve fitted) and * (measured). The inset shows a logarithmic plot for the measured intensities of an unembossed film, ▲, and a film embossed at 45° to the drawing direction, ×.

were performed for a monochromatic light source ($\lambda = 546.1$ nm) to obtain a first approximation. For the oriented polymer, based on retardation measurements, we obtained a value for δ of 13.03. Curve fitting the experimentally measured intensities resulted in values for the retardance, δ, of 12.95 for the unembossed film, and 0.06, 0.01, 0.035 for the gratings embossed, parallel, perpendicular, and at 45° to the drawing direction, respectively, (see Fig. 5c), which are lower than the with EMT calculated retardances (1.13, 0.60, 0.85). Nevertheless, the general features observed are reproduced, in particular for the "high-intensity regimes", with the above highly approximate calculations. Discrepancies in the measured data might be partly due to diffracted light. Furthermore, it is clear that for a more accurate theoretical description, more elaborate theories such as rigorous coupled-wave analysis or modal analysis have to be applied. In any case, our theoretical and experimental investigations illustrate that highly unusual birefringence effects can be generated, which may be potentially useful, for instance in optical components.

Very similar results to those presented above for FEP were obtained with a number of other, more common, semicrystalline polymers, such as linear and branched polyethylenes and poly(ethylene terephthalate). Of course, the temperatures at which single- and multiple embossing were carried out were adjusted to the appropriate ranges: that is melt-embossing and solid-state embossing at 180 °C and 90 °C for the polyethylenes; 300 °C and 90 °C for the polyester. More detailed results on studies with these materials, as well as further exploration of the use of smaller, submicrometer-structured masters will be published elsewhere.

Experimental

Films of poly(tetrafluoroethylene-*co*-hexafluoropropylene) (Teflon FEP 100, DuPont Fluoroproducts, Geneva, Switzerland; melting temperature T_m = 260 °C) with a thickness of about 200 μm were produced by compression molding at 330 °C. In addition, commercial films (Angst + Pfister, Zürich, Switzerland) were used that were drawn under constraint at elevated temperature (200 °C) to a draw ratio of about four.

A variety of silicon-based "masters" (Ultrasharp calibration gratings for SPM scanners) were purchased from NT-MTD (Moscow, Russia; area 9 mm^2). In the majority of the embossing experiments, the masters were placed onto the glass-substrate supported polymer films at room temperature. In melt-embossing experiments, the assembly was heated up to 330 °C and subjected to a pressure of 10 g/mm^2 for 5 min. Subsequently, the pressure was completely removed, the sample was quenched to room temperature and the master was lifted off. Experiments were performed at 200 °C in the case of solid-state embossing. Higher loads (300 g/mm^2 for multiple embossing, 850 g/mm^2 for embossing of oriented polymer films) and longer replication cycles (2 and 12 h) were frequently used in order to obtain homogeneously embossed relief structures over the entire sample area. Contrary to melt embossing, for these kind of experiments, the pressure was

  0935-9648/00/0804-0561 $ 17.50+.50/0

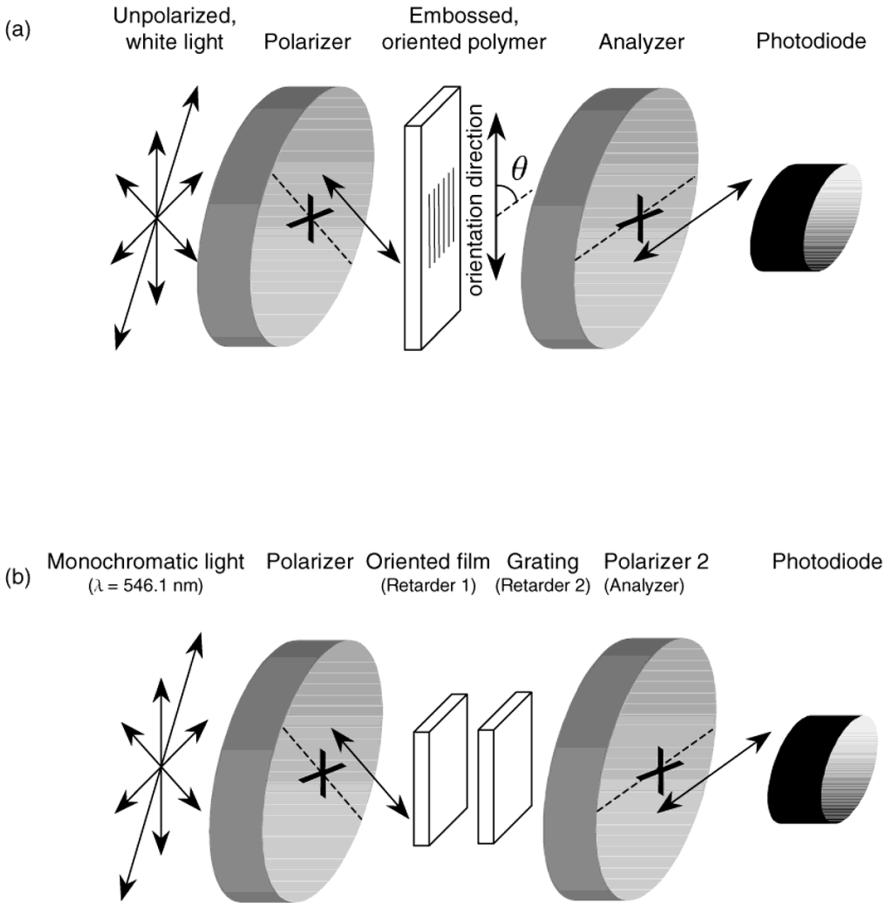

Fig. 6. Experimental set-up: a) as used for intensity measurements; b) as described theoretically.

removed only after cooling the assembly of glass substrate, polymeric film, and master to room temperature.

High-resolution optical microscopy was performed with a Leica DMRX microscope. Optical micrographs were recorded in unpolarized, reflected light of the silicon-based master and in unpolarized, transmitted light of isotropic and oriented FEP films. Also, some micrographs of oriented FEP films embossed at an angle of 45° to the drawing direction, were taken in transmitted light with crossed polarizers using a daylight filter.

Scanning probe microscopy (SPM) measurements were made with a Nanoscope IIIa Extended Multimode (Digital Instruments, Santa Barbara, CA, USA) operating the SPM in the contact mode.

Environmental scanning electron microscopy (E-SEM) was performed using a Philips FEG E-SEM XL30. Samples were prepared by mounting embossed polymer films with adhesive carbon tape onto sample holders. Low acceleration voltages (700 and 1000 V) were used to prevent charging of the polymer films.

For pattern transfer in epoxy resins, a microstructure was first melt embossed (330 °C, 5 min, 10 g/mm^2) in a FEP film. A pre-polymeric liquid, consisting of 1 mL monomer mixture (41.3 wt.-% Epon 812, Fluka: 54 wt.-% Dibutylphthalate, Fluka; 4.7 wt.-% Durcupan ACM, Fluka), 1 mL hardener (DDSA, Fluka) and 5 drops of accelerator (DMP30, Fluka), was then poured onto the microstructured polymer film and subsequently cured at 60 °C for 24 h. The epoxy replica was then removed from the FEP master.

The experimental set-up for the characterization of the optical behavior of the embossed polymer films is schematically depicted in Figure 6a. The samples were positioned between crossed linear polarizers, the drawing direction of the oriented polymer aligned at an angle, θ, with respect to the analyzer. A tungsten halogen lamp was used as a light source, its incident beam focused with a microscope lens (magnification 50×) onto the embossed grating. The transmitted light intensities for different orientation angles, θ, were measured with a highly sensitive photodiode (S2281, Hamamatsu Photonics, Japan).

The birefringence of the oriented FEP films was measured using a Leica DMRX microscope in combination with a Leitz tilting compensator. The birefringences were averaged over five measurements.

Received: October 5, 1999
Final version: January 18, 2000

[1] M. T. Gale, *Phys. World* **1989**, *2*, 24.
[2] M. T. Gale, J. Kane, K. Knop, *J. Appl. Photo. Eng.* **1978**, *4*, 41.
[3] *Holography Marketplace*, 7th ed. (Eds: A. Rhody, F. Ross), Ross Books, Berkeley, CA **1998**.
[4] E. G. Loewen, E. Popov, *Diffraction Gratings and Applications*, Marcel Dekker, New York **1997**.
[5] F. Wyrowski, E.-B. Kley, B. Schnabel, J. Turunen, M. Honkanen, M. Kuittinen, *Opt. Mem. Neural Networks* **1997**, *6*, 231.
[6] D. H. Raguin, G. M. Morris, in *Diffractive Optics: Design, Fabrication and Applications*, Vol. 11, OSA Technical Digest Series, Optical Society of America, Washington, DC **1994**, p. 252.
[7] S. J. Wilson, M. C. Hutley, *Opt. Acta* **1982**, *29*, 993.
[8] *Diffractive Optics for Industrial and Commercial Applications* (Eds: J. Turunen, F. Wyrowski), Akademie Verlag, Berlin **1997**.
[9] M. Madou, *Fundamentals of Microfabrication*, CRC Press, Boca Raton, FL **1997**.
[10] M. E. Warren, R. E. Smith, G. A. Vawter, J. R. Wendt, *Opt. Lett.* **1995**, *20*, 1441.
[11] M. T. Gale, in *Micro-Optics* (Ed: H. P. Herzig), Taylor & Francis, London **1997**, p. 153.
[12] C. Bastiaansen, H.-W. Schmidt, T. Nishino, P. Smith, *Polymer* **1993**, *34*, 3951.
[13] C.-W. Han, K. Kostuk, *J. Opt. Soc. Am. A* **1996**, *13*, 1728.
[14] S. M. Rytov, *Sov. Phys. – JETP* **1956**, *2*, 466.
[15] D. C. Flanders, *Appl. Phys. Lett.* **1983**, *42*, 492.
[16] W. Stork, N. Streibl, H. Haidner, P. Kipfer, *Opt. Lett.* **1991**, *16*, 1921.
[17] E. B. Grann, M. G. Moharam, D. A. Pommet, *J. Opt. Soc. Am. A* **1994**, *11*, 2695.
[18] L. H. Cescato, E. Gluch, N. Streibl, *Appl. Opt.* **1990**, *29*, 3286.
[19] M. Born, E. Wolf, *Principles of Optics,* 6th ed., Pergamon, Oxford **1983**, p. 703.
[20] W. A. Shurcliff, *Polarized Light: Production and Use,* Harvard University Press, Cambridge, MA **1962**, Ch. 8.
[21] G. G. Fuller, *Optical Rheometry of Complex Fluids*, Oxford University Press, New York **1995**, Ch. 8.

0935-9648/00/0804-0562 $ 17.50+.50/0